Title

Synergy of LPS and Shiga-toxin exposure on the RNA expression program of cultured human umbilical vein endothelial cells.

Abstract

Background: Hemolytic uremic syndrome (HUS) is a primary thrombotic microangiopathy that can cause acute renal failure, particularly in children, and is commonly triggered by Shiga toxin-producing *Escherichia coli* (STEC) infection. Although previous *in vitro* studies have shown that Shiga toxin (STX) can directly affect the endothelium, gram-negative bacteria such as *E. coli* also contain lipopolysaccharide (LPS) which is known to independently activate endothelial cells. Furthermore, studies in mice and baboons have shown a synergistic effect of LPS and STX in inducing HUS when administered simultaneously.
Objective: Determine how LPS, STX, or combined LPS/STX treatment affect the gene expression program of endothelial cells.
Methods: Human umbilical vein endothelial cells (HUVECs) were treated with STX, LPS or a combination of STX and LPS for either 4 or 24 hours, after which unbiased RNA sequencing analysis was performed.
Results: Four-hour treatment with LPS resulted in a greater number of differentially expressed genes as compared to treatment with STX. In contrast, 24-hour treatment with LPS or STX induced similar numbers of differentially expressed genes. Dual treatment with both toxins resulted in a synergistic effect, showing significant up- or downregulation of multiple transcripts that were not observed in either single treatment group, particularly at the 24-hour timepoint.
Conclusion: Our data provide a resource for assessing the role of endothelial cell gene expression in the pathogenesis of STEC infection and suggest that the responses of these cells to LPS, STX, or combined LPS/STX treatment are unique and temporally regulated.

Introduction

Hemolytic Uremic Syndrome (HUS) is predominantly caused by infection with Shiga-toxin (STX) producing *Escherichia coli* (STEC) O157:H7 and is the most common primary thrombotic microangiopathy (TMA) worldwide, with the majority of patients developing acute renal failure [1-3]. STX-induced damage is thought to activate microvascular endothelial cells (ECs), thereby promoting thrombotic microvascular injury in organs such as gut, kidney, brain, and heart, with renal histopathology demonstrating glomerular capillary EC thickening, swelling and luminal thrombosis [3]. STX binds EC glycosphingolipid globotriaosylceramide (Gb3), and is retrograde transported through the Golgi and endoplasmic reticulum (ER), subsequently disrupting protein synthesis leading to endothelial cell injury [4]. STX can bind circulating white blood cells, which is thought to facilitate the transfer of active STX from the gut to kidney endothelial cells [5]. Although previous studies have confirmed a key role for Gb3 receptor synthesis in STX entrance and cytotoxicity [6, 7], how STX-induced EC injury promotes HUS is still unknown.

In addition to STX, STEC also produces other toxins, including lipopolysaccharide (LPS), which is known to cause many transcriptional changes independent of STX [8]. Previous studies have shown that human

umbilical vein endothelial cell (HUVEC) survival is decreased during combined LPS and STX treatment [9, 10]. *In vivo*, LPS and STX have also been reported to have a greater than additive effect on worsening kidney function in mouse and baboon models of HUS [11, 12], with dual LPS/STX treatment of mice resulting in a greater number of significantly altered transcripts in the kidney as compared to individual LPS or STX treatment [11]. However, as this latter study evaluated changes in gene expression at the organ level, it is not possible to discern whether those changes occurred within the endothelial compartment specifically. We now report a comprehensive RNA sequencing analysis of the effects of LPS and STX in HUVECs, either alone or in combination, to mimic the early stages of STEC infection *in vivo*. We show that LPS-induced changes occur more rapidly than those induced by STX, with combined LPS/STX treatment resulting in greater than additive effects on the EC gene expression program as compared to LPS or STX alone.

Methods

Cell culture

Primary pooled HUVECs (Lonza #C2519A) were cultured in supplemented endothelial growth media-2 (Lonza EGM-2 BulletKit, #CC-3162) per the manufacturer's instructions. Holotoxin variant Shiga-toxin 2a (STX2; Phoenix Laboratory at Tufts Medical Center) was dissolved in phosphate buffered saline (PBS, Gibco #10010-023) at a stock concentration of 100 ng/uL and frozen at -80°C in single use vials that were thawed immediately prior to treatment. LPS from Escherichia coli 026:B6 was obtained from Sigma (L8274) and dissolved in PBS at a concentration of 500 µg/mL. HUVECs were seeded (passage 2; 50,000 cells/well) in 24-well plates 24 hours prior to treatment with PBS, STX (50 or 5 ng/mL), LPS (2.5 µg/mL), or combined STX and LPS.

RNA isolation and sequencing analysis

After 4 or 24 hours of treatment, cells were washed with ice cold PBS followed by RNA isolation (Takara NucleoSpin RNA) and cDNA conversion using the SMART-Seq v4 Ultra Low Input RNA Kit (Takara, #634892). Amplification, purification, cDNA shearing, and quality assessment were completed as previously described [13]. End repair, ligation, library barcoding of cDNA and subsequent amplification was performed using the KAPA HyperPrep Kit (KK8504) combined with NEXTFLEX-96 DNA Barcodes (NOVA-514105). Quality of sequencing libraries was assessed using an Agilent 2100 Bioanalyzer. Libraries were sequenced as 100 paired-end sequencing reads on the NovaSeq6000. Sequence mapping to the transcriptome (GRCh37 human version 32) and quantification was performed using Salmon [14], and the resulting output was directly loaded into DESeq2 using tximport for downstream normalization and differential expression analysis [15, 16]. An average raw read count of 20 per sample was used to filter out very low expression transcripts to reduce background noise prior to differential expression analysis. The transcripts that were below the filter threshold were predominantly non-protein coding (16.2%). In contrast, transcripts above the filter threshold were primarily protein coding (87.1%), suggesting the filter was effective at removing background noise while capturing significant gene expression changes. A false discovery rate [17] (FDR or q-value) of <0.05 in combination with a log2 fold change <-1 or >1 was used to define statistically significant differential gene expression. Gene Ontology (GO) analysis was performed on gene lists passing the above statistical threshold using the "Search Tool for Retrieval of Interacting Genes/Proteins" (STRING) database [18]. Data visualization was performed

using R, and Venn diagrams were created online using http://bioinformatics.psb.ugent.be/webtools/Venn/.

Reanalysis of STX treated HUVEC microarray data
Microarray data from a previous study where human micro vascular endothelial cells (HMVECs) were treated with STX ([19]; Gene Expression Omnibus GSE32710) was accessed and reanalyzed using the GEO2R webtool, with the same statistical cutoffs used for our RNA sequencing data (FDR <0.05 and log2-fold-change >1 or <-1) [20, 21].

Results and Discussion

STX- and LPS-induced gene expression changes exhibit significant overlap with slower onset for STX
RNA-seq data from HUVECs treated with STX or LPS were highly reproducible between biological replicates (Fig 1A). Approximately 20% of the total genes evaluated were differentially expressed (2804 genes of 14245 total genes) at 4-hours compared to 24-hour PBS-treated control HUVECs in cell culture. GO analysis [18] of significantly downregulated genes (1871 / 14245 total # of genes) showed enrichment for biological processes focused on vascular development and proliferation, consistent with the expected senescence observed in primary cells during increased time in culture [22] and the phenotypic drift previously reported for primary ECs grown in culture after being removed from their *in vivo* microenvironment [13]. Therefore, all subsequent analyses were performed using vehicle treated controls at the same timepoint as the reference to distinguish toxin-induced changes in gene expression.

Upregulated genes composed the majority of the significantly affected genes by toxin treatment at both time points (Figure 2 A-F). STX treatment at either 5 or 50 ng/ml resulted in extensive overlap and could not be differentiated by PCA at the 4-hour time point (Figure 1B, C). Due to the increased gene expression changes at 24h with STX 50ng/mL, we focus our analysis on this treatment group. LPS induced rapid changes in mRNA expression, with 880 differentially expressed genes observed after 4-hour treatment, whereas only 318 genes were differentially expressed after STX treatment at 4-hours. Significant overlap was observed in STX and LPS induced differential gene expression with 990 out of 3536 unique genes being present in both treatment groups at 24-hours (Figure 2G, H).
GO analysis of the 500 genes with the lowest q-values after LPS treatment was conducted to assess enriched biological processes. Analysis of differentially expressed genes after 4-hour LPS treatment yielded GO terms related to vascular wound healing, response to IL-18, regulation of IL-1 and TGF-B and sequestration of NF-kB. GO analysis for 24-hour LPS treatment revealed overrepresentation of genes involved in expected pathways related to inflammation (Figure 3), as the consequence of the upregulation of genes associated with endothelial cell activation [23]. In contrast, STX treatment resulted in significantly upregulated transcripts overrepresented in GO terms focusing on the ER stress response and p38/MAPK signaling at 24 hours (Figure 4). This is potentially due to STX-mediated protein synthesis inhibition inducing ER stress, consistent with previously reported findings that p38/MAPK signaling is essential for STX-induced increases in macrophage cytokine production [24, 25]. ECs have been shown to increase cytokine production in response to bacterial toxins such as STX and LPS [26] and thus may also require p38/MAPK signaling to increase cytokine production. In our data, TNF and IL6 are significantly upregulated with LPS treatment at 4-hours (more pronounced at 24-hours), but not with STX treatment alone. Prior studies have shown that TNF and IL6 levels correlate with HUS severity and

development of extrarenal complications, suggesting that the LPS-induced inflammatory response in STEC infection likely contributes to HUS development[27].
Since ECs are highly heterogeneous, we asked whether our findings could be applicable to ECs from different tissue origins by comparing our HUVEC data to a previously published study characterizing the response to 24-hour STX treatment in HMVECs, as evaluated by microarray analysis [19]. Although only 57 genes showed statistically significant differences in HMVECs, 35 of these genes overlap with our 24h STX treatment data. GO analysis of these 35 transcripts also identified enrichment for regulation of the p38MAPK cascade, suggesting that this pathway is part of a general response to STX that is independent of EC origin.

Combined STX and LPS treatment synergistically induces differential gene expression not observed in individual treatments

STEC produces both LPS and STX, and previous studies have demonstrated that combined LPS/STX treatment has a greater than additive effect on HUVEC cell survival and worsening kidney function in animal models of HUS [9-11]. Concurrent treatment of HUVEC with LPS and STX induced significant expression changes in a subset of genes which were uniquely altered only in the combined treatment (1364 out of 3308 total differentially expressed genes; Figure 2). Pathway analysis of genes upregulated with dual STX/LPS treatment revealed enrichment of unfolded protein response, p38MAPK, NFκB, and p-ERK signaling. Transcripts downregulated by LPS/STX were associated with DNA repair and replication (Figure 3). This latter finding suggests a decrease in cellular replication, which corresponds with a prior report demonstrating that STX-treated cells slow their cell cycle progression[28].
LPS facilitates STX binding to the cell surface by increasing Gb3 receptor expression in specific EC populations, including HUVECs [9]. In our study, there was a significant increase in both *UGCG* and *B4GALT5* with LPS treatment, the 2 enzymes preceding the final enzyme to synthesize Gb3, *A4GALT*. However, there was no significant difference in *A4GALT* expression in any of the treatment conditions. Therefore, it is possible that the previously reported increase in Gb3 in HUVECs after LPS treatment is due to differential expression of *UGCG* and *B4GALT5*, but not *A4GALT* and may confer additional STX sensitivity with dual treatment. Of note, renal ECs, the presumed STX target in HUS, have been reported to express 50x higher Gb3 at baseline and are more sensitive to STX than HUVECs, yet do not exhibit an increase in Gb3 or STX binding following LPS treatment [9]. However, dual LPS/STX treatment was synergistic in inducing HUS in both mouse [11, 29] and baboon models [12], suggesting that LPS treatment is conferring additional kidney EC sensitivity despite significant Gb3 receptor present at baseline on renal ECs.
Although STX-induced expression changes are delayed as compared to LPS effects, this might mimic the clinical manifestation as diarrhea typically occurs 3 days after ingestion of STEC, with HUS developing after approximately 7 days of diarrhea [1]. Therefore, the synergistic differential gene expression changes may be responsible for the delay in TMA development. Some gene expression changes that may impact HUS pathogenesis include the IL10 and IL18 signaling pathways that were upregulated in our 24-hour LPS treatment. A prior study demonstrated that IL10 deficient mice exhibit increased survival in an HUS mouse model compared to control mice [30]. Thus, LPS-induced IL10 secretion may contribute to LPS/STX synergistic toxicity. Potential additional mechanisms include LPS induced inflammation, thereby promoting increased white blood cell delivery of STX to the kidney, leading to renal EC STX-induced damage and HUS[5]. With both LPS and STX present during STEC infection, our

data characterizing the synergistic EC expression changes with dual LPS/STX treatment provide a valuable resource for future examination of the pathophysiology of HUS and may represent a more accurate model of STEC induced differential gene expression than exposure to LPS or STX alone.

References

1 Tarr PI, Gordon CA, Chandler WL. Shiga-toxin-producing Escherichia coli and haemolytic uraemic syndrome. *Lancet*. 2005; **365**: 1073-86. 10.1016/S0140-6736(05)71144-2.

2 Flynn JT. Causes, management approaches, and outcome of acute renal failure in children. *Curr Opin Pediatr*. 1998; **10**: 184-9. 10.1097/00008480-199804000-00012.

3 Freedman SB, van de Kar NCAJ, Tarr PI. Shiga Toxin-Producing. *N Engl J Med*. 2023; **389**: 1402-14. 10.1056/NEJMra2108739.

4 Tsai HM. The molecular biology of thrombotic microangiopathy. *Kidney Int*. 2006; **70**: 16-23. 10.1038/sj.ki.5001535.

5 Niu S, Paluszynski J, Bian Z, Shi L, Kidder K, Liu Y. LPS-primed CD11b+ leukocytes serve as an effective carrier of Shiga toxin 2 to cause hemolytic uremic syndrome in mice. *Sci Rep*. 2018; **8**: 3994. 10.1038/s41598-018-22327-4.

6 Pacheco AR, Lazarus JE, Sit B, Schmieder S, Lencer WI, Blondel CJ, Doench JG, Davis BM, Waldor MK. CRISPR Screen Reveals that EHEC's T3SS and Shiga Toxin Rely on Shared Host Factors for Infection. *MBio*. 2018; **9**. 10.1128/mBio.01003-18.

7 Yamaji T, Sekizuka T, Tachida Y, Sakuma C, Morimoto K, Kuroda M, Hanada K. A CRISPR Screen Identifies LAPTM4A and TM9SF Proteins as Glycolipid-Regulating Factors. *iScience*. 2019; **11**: 409-24. 10.1016/j.isci.2018.12.039.

8 Mullins GE, Sunden-Cullberg J, Johansson AS, Rouhiainen A, Erlandsson-Harris H, Yang H, Tracey KJ, Rauvala H, Palmblad J, Andersson J, Treutiger CJ. Activation of human umbilical vein endothelial cells leads to relocation and release of high-mobility group box chromosomal protein 1. *Scand J Immunol*. 2004; **60**: 566-73. 10.1111/j.0300-9475.2004.01518.x.

9 Obrig TG, Louise CB, Lingwood CA, Boyd B, Barley-Maloney L, Daniel TO. Endothelial heterogeneity in Shiga toxin receptors and responses. *J Biol Chem*. 1993; **268**: 15484-8.

10 Louise CB, Obrig TG. Shiga toxin-associated hemolytic uremic syndrome: combined cytotoxic effects of shiga toxin and lipopolysaccharide (endotoxin) on human vascular endothelial cells in vitro. *Infect Immun*. 1992; **60**: 1536-43.

11 Keepers TR, Psotka MA, Gross LK, Obrig TG. A murine model of HUS: Shiga toxin with lipopolysaccharide mimics the renal damage and physiologic response of human disease. *J Am Soc Nephrol*. 2006; **17**: 3404-14. 10.1681/ASN.2006050419.

12 Siegler RL, Pysher TJ, Lou R, Tesh VL, Taylor FB. Response to Shiga toxin-1, with and without lipopolysaccharide, in a primate model of hemolytic uremic syndrome. *Am J Nephrol*. 2001; **21**: 420-5. 10.1159/000046288.

13 Cleuren ACA, van der Ent MA, Jiang H, Hunker KL, Yee A, Siemieniak DR, Molema G, Aird WC, Ganesh SK, Ginsburg D. The in vivo endothelial cell translatome is highly heterogeneous across vascular beds. *Proc Natl Acad Sci U S A*. 2019; **116**: 23618-24. 10.1073/pnas.1912409116.

14 Patro R, Duggal G, Love MI, Irizarry RA, Kingsford C. Salmon provides fast and bias-aware quantification of transcript expression. *Nat Methods*. 2017; **14**: 417-9. 10.1038/nmeth.4197.

15 Soneson C, Love MI, Robinson MD. Differential analyses for RNA-seq: transcript-level estimates improve gene-level inferences. *F1000Res*. 2015; **4**: 1521. 10.12688/f1000research.7563.2.

16 Love MI, Huber W, Anders S. Moderated estimation of fold change and dispersion for RNA-seq data with DESeq2. *Genome Biol*. 2014; **15**: 550. 10.1186/s13059-014-0550-8.

17 Benjamini Y, Hochberg Y. Controlling the False Discovery Rate: A Practical and Powerful Approach to Multiple Testing. *Journal of the Royal Statistical Society Series B (Methodological)*. 1995; **57**: 289-300.
18 Szklarczyk D, Kirsch R, Koutrouli M, Nastou K, Mehryary F, Hachilif R, Gable AL, Fang T, Doncheva NT, Pyysalo S, Bork P, Jensen LJ, von Mering C. The STRING database in 2023: protein-protein association networks and functional enrichment analyses for any sequenced genome of interest. *Nucleic Acids Res*. 2023; **51**: D638-D46. 10.1093/nar/gkac1000.
19 Petruzziello-Pellegrini TN, Yuen DA, Page AV, Patel S, Soltyk AM, Matouk CC, Wong DK, Turgeon PJ, Fish JE, Ho JJ, Steer BM, Khajoee V, Tigdi J, Lee WL, Motto DG, Advani A, Gilbert RE, Karumanchi SA, Robinson LA, Tarr PI, Liles WC, Brunton JL, Marsden PA. The CXCR4/CXCR7/SDF-1 pathway contributes to the pathogenesis of Shiga toxin-associated hemolytic uremic syndrome in humans and mice. *J Clin Invest*. 2012; **122**: 759-76. 10.1172/JCI57313.
20 Barrett T, Wilhite SE, Ledoux P, Evangelista C, Kim IF, Tomashevsky M, Marshall KA, Phillippy KH, Sherman PM, Holko M, Yefanov A, Lee H, Zhang N, Robertson CL, Serova N, Davis S, Soboleva A. NCBI GEO: archive for functional genomics data sets--update. *Nucleic Acids Res*. 2013; **41**: D991-5. 10.1093/nar/gks1193.
21 Edgar R, Domrachev M, Lash AE. Gene Expression Omnibus: NCBI gene expression and hybridization array data repository. *Nucleic Acids Res*. 2002; **30**: 207-10. 10.1093/nar/30.1.207.
22 Hayflick L, Moorhead PS. The serial cultivation of human diploid cell strains. *Experimental Cell Research*. 1961; **25**: 585-621. https://doi.org/10.1016/0014-4827(61)90192-6.
23 Albrecht EA, Chinnaiyan AM, Varambally S, Kumar-Sinha C, Barrette TR, Sarma JV, Ward PA. C5a-induced gene expression in human umbilical vein endothelial cells. *Am J Pathol*. 2004; **164**: 849-59. 10.1016/S0002-9440(10)63173-2.
24 van Setten PA, Monnens LA, Verstraten RG, van den Heuvel LP, van Hinsbergh VW. Effects of verocytotoxin-1 on nonadherent human monocytes: binding characteristics, protein synthesis, and induction of cytokine release. *Blood*. 1996; **88**: 174-83.
25 Cherla RP, Lee SY, Mees PL, Tesh VL. Shiga toxin 1-induced cytokine production is mediated by MAP kinase pathways and translation initiation factor eIF4E in the macrophage-like THP-1 cell line. *J Leukoc Biol*. 2006; **79**: 397-407. 10.1189/jlb.0605313.
26 Shao Y, Saredy J, Yang WY, Sun Y, Lu Y, Saaoud F, Drummer C, Johnson C, Xu K, Jiang X, Wang H, Yang X. Vascular Endothelial Cells and Innate Immunity. *Arterioscler Thromb Vasc Biol*. 2020; **40**: e138-e52. 10.1161/ATVBAHA.120.314330.
27 Fernández GC, Ramos MV, Landoni VI, Bentancor LV, Fernández-Brando RJ, Exeni R, Laso MeC, Exeni A, Grimoldi I, Isturiz MA, Palermo MS. Cytokine production is altered in monocytes from children with hemolytic uremic syndrome. *J Clin Immunol*. 2012; **32**: 622-31. 10.1007/s10875-011-9646-z.
28 Suardana IW, Swacita IBN, Pinatih KJP, Suharsono H, Widiasih DA. Assessment of Cell Cycle and Induction of Apoptosis by Shiga-like Toxin Produced by Escherichia coli O157:H7 in T47D Breast Cancer Cells Using Flow Cytometry. *Asian Pac J Cancer Prev*. 2022; **23**: 3247-52. 10.31557/APJCP.2022.23.10.3247.
29 Ikeda M, Ito S, Honda M. Hemolytic uremic syndrome induced by lipopolysaccharide and Shiga-like toxin. *Pediatr Nephrol*. 2004; **19**: 485-9. 10.1007/s00467-003-1395-7.
30 Pineda GE, Rearte B, Todero MF, Bruballa AC, Bernal AM, Fernandez-Brando RJ, Isturiz MA, Zotta E, Alba-Soto CD, Palermo MS, Ramos MV. Absence of interleukin-10 reduces progression of shiga toxin-induced hemolytic uremic syndrome. *Clin Sci (Lond)*. 2021; **135**: 575-88. 10.1042/CS20200468.

Figure Legends:

Figure 1: HUVECs treated with STX, LPS or dual treatment exhibit significant overlap of differentially expressed genes. Principal component analysis of vehicle, STX, LPS, and combined STX/LPS treatment at both (A) 4 and 24-hours, (B) 4-hours, or (C) 24-hours only. Heatmap plotting the log2 fold change compared to vehicle controls, across treatments (columns) and individual genes (rows) for (D) 4-hours and (E) 24-hour treatment.

Figure 2: Volcano plots with differential expression on the x-axis (log2 fold change of experimental compared to control), and statistical significance on the y-axis (-log10 of the q-value) were plotted. Dashed lines demarcate the statistical cutoffs (log2 fold change <-1 or >1, q-value <0.05). Significantly differentially expressed genes (red), and not significant genes (gray) for (A) STX 50nm at 4-hours, (B) STX 50nm and LPS at 4-hours, (C) LPS at 4-hours, (D) STX 50nm at 24-hours, (E) STX 50nm and LPS at 24-hours, and (F) LPS at 24-hours were plotted. The volcano plots were truncated at a q-value of 10^{-125} to enable better visualization of the rest of the graph that was otherwise compressed by the most significantly differentially expressed genes. Genes that that were truncated off the volcano plot are listed in Supplemental Table 1. Venn diagrams display the overlap of differentially expressed genes between the different treatments compared to PBS controls at (G) 4-hours and 24-hours (H).

Figure 3: GO terms enriched for inflammatory related biological processes after 24-hour LPS treatment, upregulated secondary to endothelial cell activation with the associated false discovery rates and genes responsible for the biological enrichment.

Figure 4: GO terms enriched in ER stress response and p38/MAPK signaling biological processes after 24-hour STX treatment.

Supplemental Figure 1: Volcano plots of HUVECs treated with both STX 5nm and LPS at 4-hours (A) and 24-hours (B) demonstrate increased differential gene expression compared to individual STX or LPS treatments at both time points, with color denoting significantly differentially expressed (red), or not significant genes (gray).

Figure 1

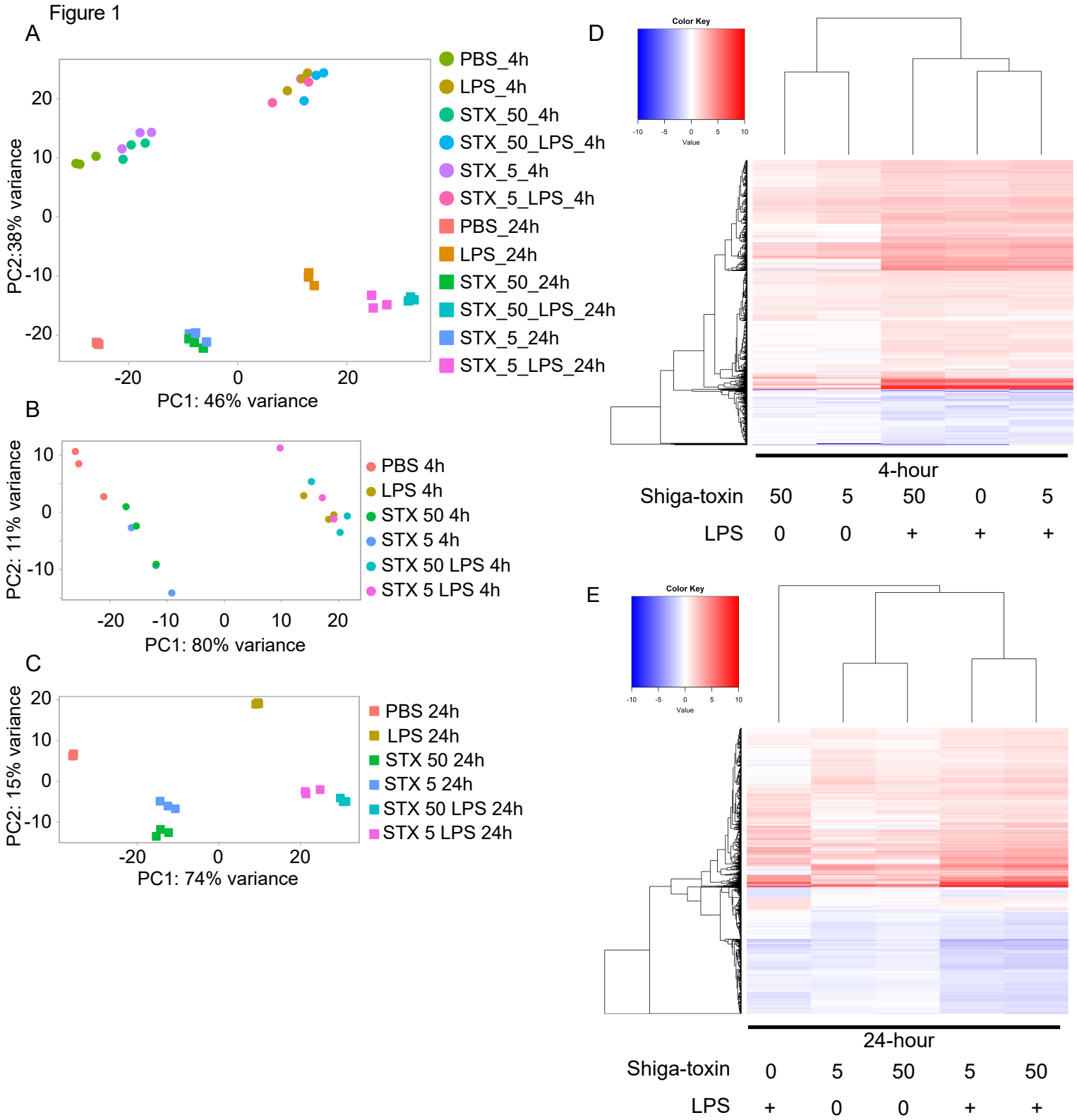
A
PC2:38% variance
PC1: 46% variance
PBS_4h
LPS_4h
STX_50_4h
STX_50_LPS_4h
STX_5_4h
STX_5_LPS_4h
PBS_24h
LPS_24h
STX_50_24h
STX_50_LPS_24h
STX_5_24h
STX_5_LPS_24h
B
PC2: 11% variance
PC1: 80% variance
PBS 4h
LPS 4h
STX 50 4h
STX 5 4h
STX 50 LPS 4h
STX 5 LPS 4h
C
PC2: 15% variance
PC1: 74% variance
PBS 24h
LPS 24h
STX 50 24h
STX 5 24h
STX 50 LPS 24h
STX 5 LPS 24h
D
Color Key
Value
4-hour
Shiga-toxin 50 5 50 0 5
LPS 0 0 + + +
E
Color Key
Value
24-hour
Shiga-toxin 0 5 50 5 50
LPS + 0 0 + +

Figure 2

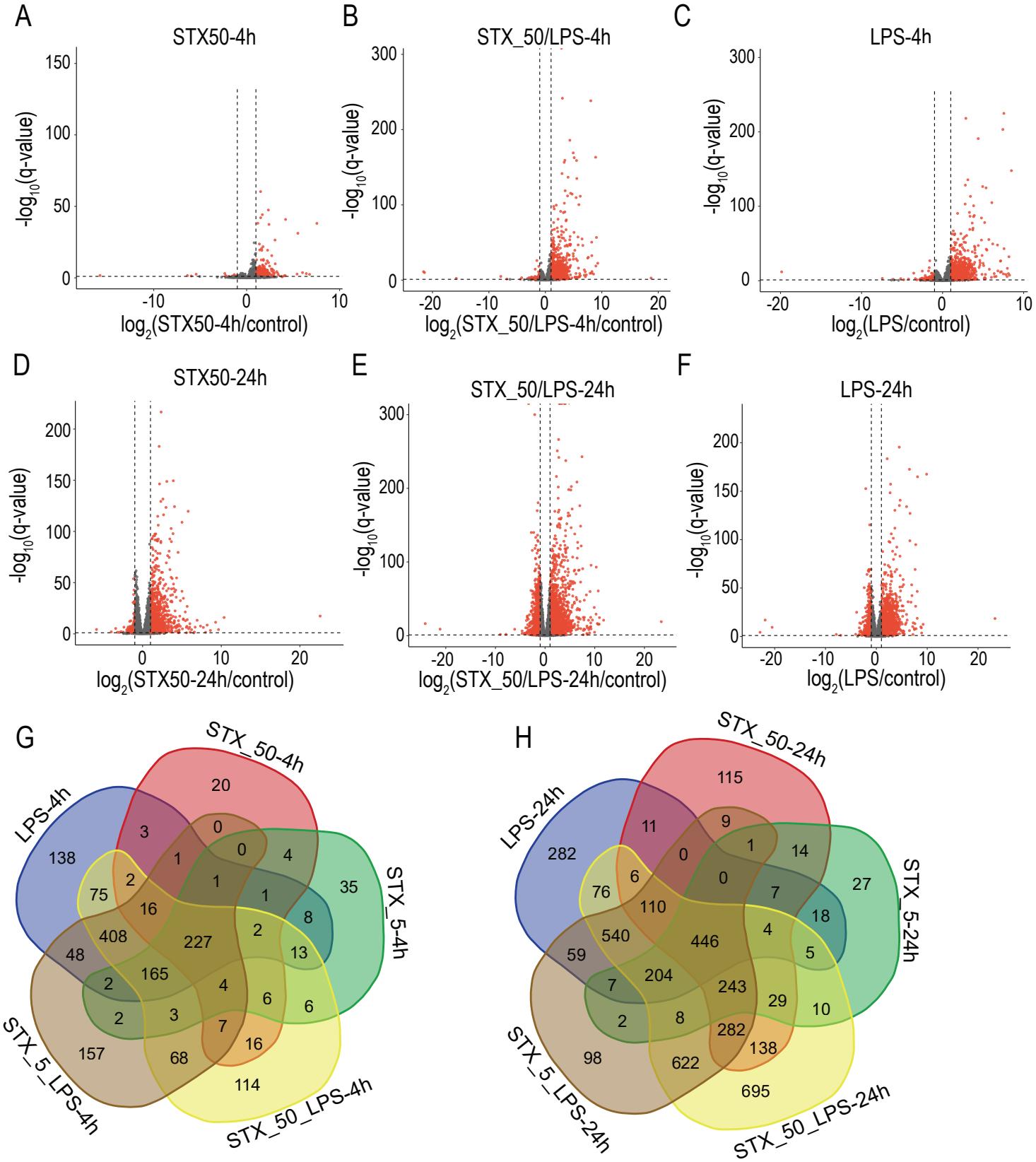
A
STX50-4h
-log10(q-value)
log2(STX50-4h/control)
B
STX_50/LPS-4h
-log10(q-value)
log2(STX_50/LPS-4h/control)
C
LPS-4h
-log10(q-value)
log2(LPS/control)
D
STX50-24h
-log10(q-value)
log2(STX50-24h/control)
E
STX_50/LPS-24h
-log10(q-value)
log2(STX_50/LPS-24h/control)
F
LPS-24h
-log10(q-value)
log2(LPS/control)
G
STX_50-4h
LPS-4h
STX_5-4h
STX_5_LPS-4h
STX_50_LPS-4h
20
3
0
0
4
138
1
1
1
35
75
2
16
8
408
227
2
13
48
165
2
4
6
6
2
3
7
16
157
68
114
H
STX_50-24h
LPS-24h
STX_5-24h
STX_5_LPS-24h
STX_50_LPS-24h
115
11
9
1
14
282
0
0
27
76
6
7
110
18
540
446
4
5
59
204
243
29
10
7
2
8
282
138
98
622
695

Figure 3

GO term description	Enrichment strength	proteins in network
Response to interleukin-18	1.37	RIPK2,CLDN1,PDGFB,IL18R1
Receptor-mediated virion attachment to host cell	1.24	CD81,ICAM1,GAS6
Positive regulation of microglial cell migration	1.24	CX3CL1,CSF1,P2RX4
Endothelial cell activation	1.17	TCIM,P2RX4,TGFBR1,FOXP1
Positive regulation of p38MAPK cascade	0.96	GDF6,STK39,MAP3K5,MAP3K3,ZC3H12A,BMP2
Positive regulation of macrophage derived foam cell differentiation	0.96	NFKB1,CSF2,CSF1,MAPK9

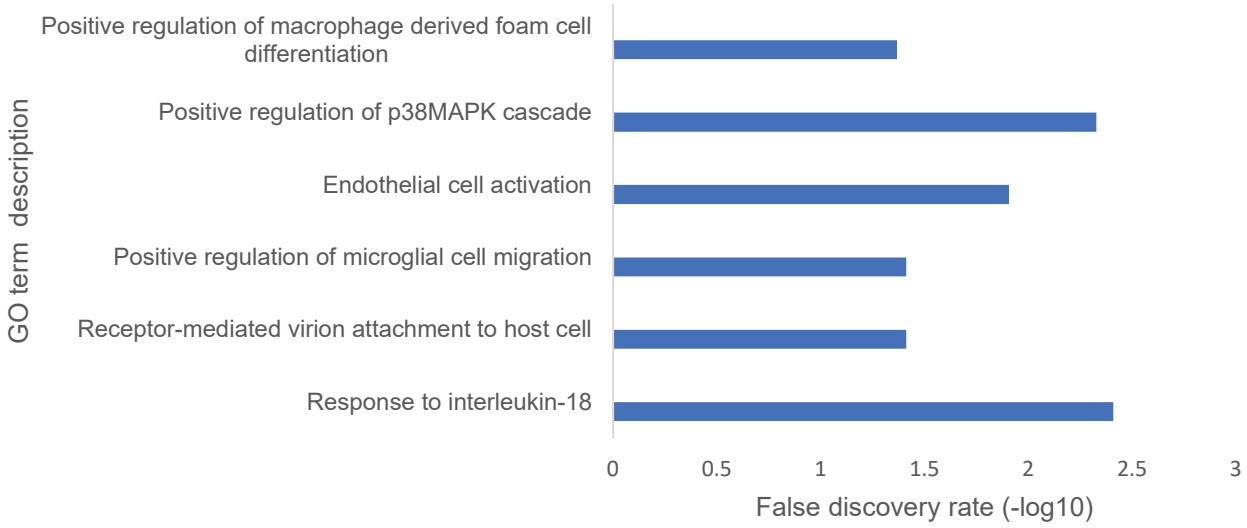

Figure 4
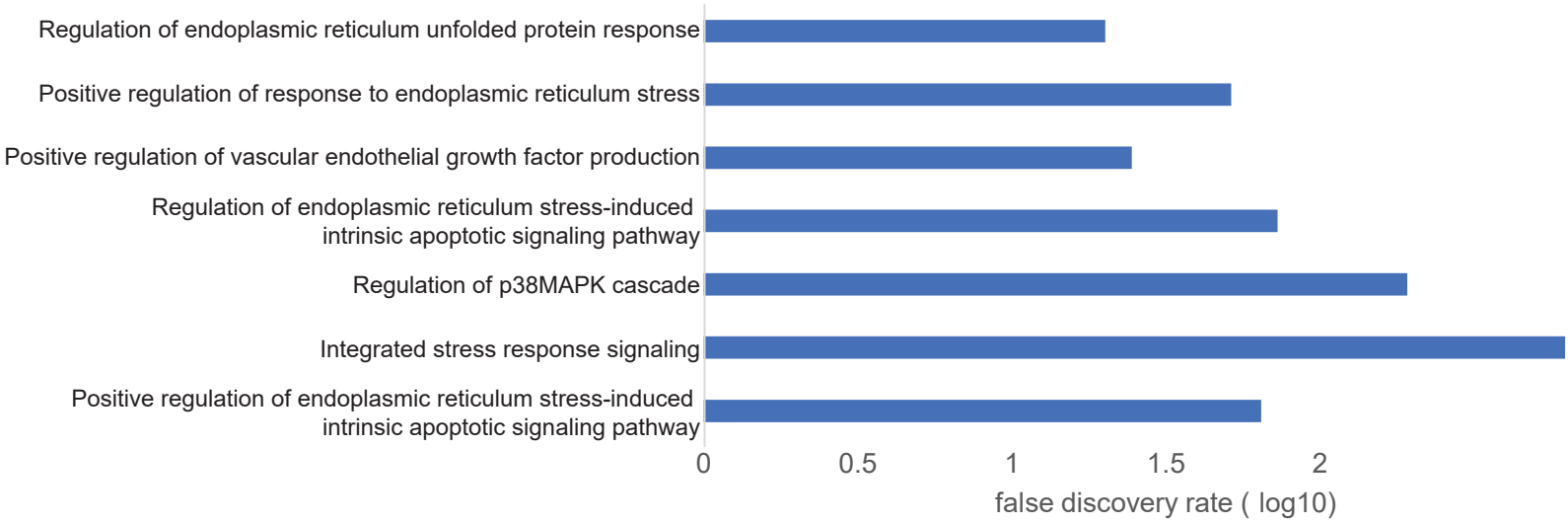
GO term description	Strength of enrichment	Proteins in network
Positive regulation of endoplasmic reticulum stress-induced intrinsic apoptotic signaling pathway	1.21	SIRT1,PMAIP1,BBC3,DDIT3
Integrated stress response signaling	1	JUNB,FOS,EIF2AK3,FOSL1,ATF4,CEBPD,DDIT3
Regulation of p38MAPK cascade	0.89	GADD45B,DUSP1,PER1,DUSP10,GADD45A,BMP2,CYLD
Regulation of endoplasmic reticulum stress-induced intrinsic apoptotic signaling pathway	0.89	SIRT1,EIF2AK3,PMAIP1,PTPN1,BBC3,DDIT3
Positive regulation of vascular endothelial growth factor production	0.88	IL1A,EIF2AK3,ATF4,IL6,CYP1B1
Positive regulation of response to endoplasmic reticulum stress	0.86	SIRT1,PMAIP1,PTPN1,ERN1,BBC3,DDIT3
Regulation of endoplasmic reticulum unfolded protein response	0.86	PPP1R15A,CREBRF,PTPN1,ERN1,BBC3